Communication

Synthesis of Square Gadolinium-Oxide Nanoplates

Y. Charles Cao

J. Am. Chem. Soc., **2004**, 126 (24), 7456-7457• DOI: 10.1021/ja0481676 • Publication Date (Web): 27 May 2004

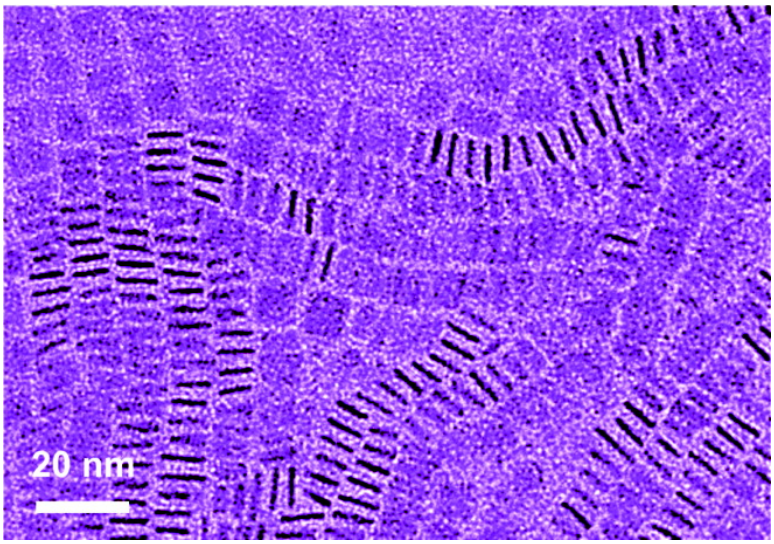

J|A|C|S
COMMUNICATIONS

Published on Web 05/27/2004

Synthesis of Square Gadolinium-Oxide Nanoplates

Y. Charles Cao

Department of Chemistry, University of Florida, Gainesville, Florida 32611

Received March 30, 2004; E-mail: cao@chem.ufl.edu

The synthesis of anisotropic nanocrystals such as nanorods, nanowires, nanotubes, and nanodisks is of great importance to applications ranging from chemical and biological sensing, separation, and catalysis to lasers and LEDs.[1,2] The formation of the anisotropic nanostructures is achieved by shape control in the crystallization process that includes nucleation and growth. In colloidal synthesis, several parameters (e.g., ligands, precursors, and reaction temperature) have been chosen to affect the kinetics and thermodynamics in the nucleation and growth of nanocrystals, achieving shape control, which has led to the synthesis of a variety of nanorods and nanowires, as well as PbS nanostars, Ag cubes, and tetrapod-shaped CdTe nanocrystals.[3−5]

However, less is known about the colloidal synthesis for plate-shaped nanocrystals, except for Co, TiO_2, Cu_2S, and NiS nanodisks and Ag nanodisks and nanoprisms.[6] Herein, we report a colloidal synthesis of square, plate-shaped gadolinium-oxide nanocrystals. These nanoplates are highly uniform and simultaneously form superlattice (SP) structures via a self-organization process.

The gadolinium-oxide nanocrystals were synthesized by solution-phase decomposition of gadolinium-acetate precursors in the presence of both coordinating and noncoordinating solvents. In a typical experiment, gadolinium acetate hydrate (0.75 mmol, from Aldrich) was dissolved in a solution that contained oleylamine (1.7 mL), oleic acid (1 mL), and octadecene (2.7 mL) at 100 °C with vigorous stirring under vacuum (~20 mTorr). Under Ar flow, the resulting solution was heated to 320 °C over approximately 5 min, and then the solution was cooled to room temperature after 1 h. The nanocrystals were precipitated from the reaction solution by adding a mixture of hexane and acetone (1:4) and dried under an Ar flow. The as-prepared nanocrystals are dispersible in nonpolar organic solvents such as toluene and hexane.

X-ray powder diffraction (XRD) indicated that the nanocrystals consist of crystalline Gd_2O_3. The wide-angle XRD pattern of the nanocrystals shows the characteristic peaks of the cubic Gd_2O_3 crystal phase, which are broadened because of the finite crystalline domain size (Figure 1A). This cubic phase has a bixbyite crystal structure with a space group Ia3 and a lattice constant of 1.08 nm. The unit cell of Gd_2O_3 is large and contains 80 atoms, which can be viewed as an ordered super-cell of fluorite structure with the gadolinium cations occupying the positions of the calcium cations.[7]

Transmission electron microscopy (TEM, JEOL-JEM 2010 operated at 200 kV) shows that the Gd_2O_3 nanocrystals are indeed square nanoplates rather than cubes. The edge length of each nanoplate is 8.1 nm with a standard deviation of 6% (Figure 1C−F). Interestingly, upon evaporation of the solvent, the Gd_2O_3 nanoplates assemble into "stacks" on the TEM grids, which lead to ribbons of stacked plates lying on edge (Figure 1D). The face-to-face position of the stacked standing plates allows for a measurement of their thickness. Amazingly, the thicknesses of these nanoplates are identical, approximately 1.1 nm.

High-resolution TEM (HRTEM) was used to further investigate the crystal structure of the nanoplates. With the nanoplates lying on their faces, no clear lattice fringes were observed, which is partially because the plates are too thin (~1.1 nm) to generate a clear contrast against the carbon film. However, the lattice fringes were evident with the nanoplates standing on their edges. Along the thickness of the nanoplates, unusual double-lattice fringes were clearly revealed, indicating a two-layer periodicity of atomic arrangement (Figure 2). The corresponding lattice planes could be assigned to the (002) planes with an interplanar distance of 0.54 nm. Observing perpendicular to the thickness of the nanoplates, lattice fringes have an interplanar distance of 0.27 nm, correspond-

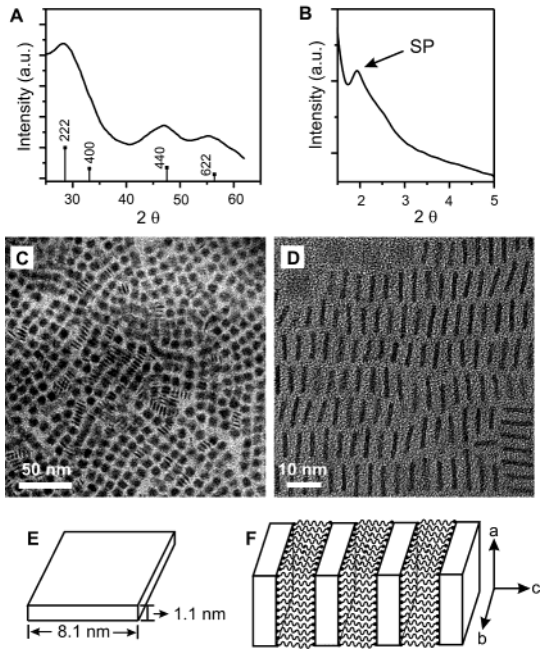

Figure 1. (A) Wide-angle XRD. The standard diffraction peak positions of bulk cubic Gd_2O_3 are indicated. (B) Small-angle XRD. (C and D) TEM images of Gd_2O_3 nanoplates. (E and F) Proposed model for the nanoplates and assembly of nanoplate stacks, respectively. The *c*-axis of cubic Gd_2O_3 crystals is assigned as the thickness direction of the nanoplates.

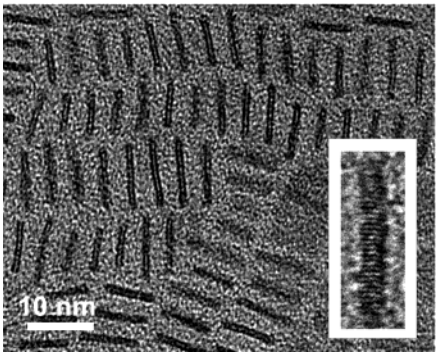

Figure 2. HRTEM image of Gd_2O_3 nanoplates. The insert is the cross-fringe image.

10.1021/ja0481676 CCC: $27.50

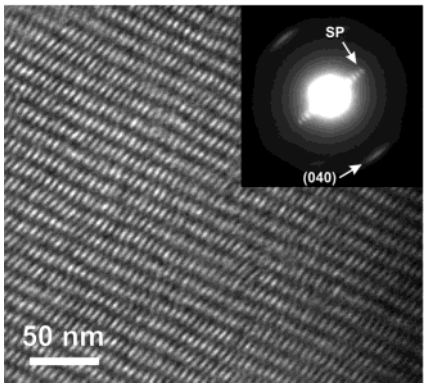

Figure 3. TEM image of the superlattice of Gd_2O_3 nanoplates. The insert is an electron-diffraction pattern taken in this area.

ing to the lattice spacing of either (400) or (040) planes (Figure 2 insert). Taken together, these data are consistent with a crystal structure model for the nanoplate, which is enclosed by the {100} faces with the *c*-axis as the direction of the thickness, where the sides of a nanoplate are enclosed by the ±(100) and ±(010) faces and the top and bottom by the ±(001) faces. Therefore, the thickness of each nanoplate is the edge length of one unit cell of cubic Gd_2O_3 (1.08 nm), which is consistent with the direct measurement of the nanoplate thickness (~1.1 nm).

Since the nanoplates have a cubic crystal structure, crystal symmetries along *a*-, *b*-, and *c*-axes should be equivalent. Then, we would expect to see the same lattice fringes shown along all three directions, but instead we see the lattice fringes along the *c*-axis related to the (002) planes, while the finer fringes along the *a*- and *b*-axes are related to the (400) and (040) planes, respectively. This discrepancy can be resolved using the above crystal structure model for the nanoplates. Along the *c*-axis, the nanoplates have only one unit cell of Gd_2O_3, with the top and bottom (001) faces modified by the organic ligands, which leads to the crystal discontinuity on these crystal faces. Therefore, the (004) lattice planes close to the top and bottom faces are no longer the glide planes in the nanoplates, causing the symmetry breakdown of these (004) crystal planes. Consequently, the (004) fringes vanish, while the (002) fringes are revealed, partially because the (002) planes are still the mirror planes in the nanoplates. This is a reverse process of the systematic absence of Bragg reflections caused by the loss of glide planes due to crystal size confinement. This size confinement does not exist along the *a*- and *b*-axes of the nanoplates because their dimensions (~8.1 nm) are much larger than the size of the unit cell. Therefore, the lattice fringes corresponding to the (400) and (040) faces are still evident.

Moreover, the above results are consistent with those of electron diffraction (ED). The high uniformity of these nanoplates allows the formation of superlattices. Superlattices in sizes from one micron to tens of microns were generated by slow evaporation of a concentrated nanoplate solution (toluene/hexane = 1/1) on TEM grids (Figure 3). Two sets of the diffraction spots shown in the ED pattern indicate a highly ordered superlattice structure of the nanoplates (Figure 3 insert). The closer diffraction spots represent a periodicity length of 4.2 nm, corresponding to the interparticle distance in the nanoplate superlattice, which is consistent with TEM and small-angle XRD measurements (Figure 1). The other set of diffraction spots represents an order distance of 0.27 nm, corresponding to the lattice spacing of (040) in the nanoplates. These ED data provide further evidence for the structural mode of the nanoplates (Figure 1 f). The direction of the nanoplate stacking is along the *c*-axis, perpendicular to the *a*- and *b*-axes of the plates. Consequently, the two sets of diffraction spots are perpendicular, as shown in the ED pattern.

To gain further insight into the growth mechanism of these Gd_2O_3 nanoplates, we have investigated a series of growth solvents. The use of oleylamine alone during the reaction resulted in white precipitates that were insoluble in nonpolar solvents. On the other hand, the use of oleic acid alone produced very small particles (~2 nm). In the presence of both oleylamine and oleic acid, the reactions yielded nanoplates with broad distributions in size and shape (Supporting Information). When octadecene, a noncoordinating solvent, is introduced into the oleylamine and oleic acid mixture, the reactions led to nanoplates with very narrow size and shape distributions. These results indicate the necessity of the three-solvent combination for the synthesis of high-quality nanoplates. However, these results cannot explain the formation of plate-shaped nanocrystals, which should be caused by the symmetry breaking between the {100} faces during the gadolinium-oxide nanocrystal's growth. Although the detailed mechanism remains to be developed, it is highly possible that the crystal growth habit of gadolinium oxide plays a significant role. Indeed, similar phenomena on the symmetry breaking between the equivalent crystal faces have been observed in the synthesis of multi-micron-length metal-oxide nanobelts and nanowires.[8]

In conclusion, this paper reports a solution-phase synthesis of high-quality, square, plate-shaped Gd_2O_3 nanocrystals. These nanoplates are single crystalline with a thickness of the Gd_2O_3 unit-cell edge length, approaching the lower limit of crystal growth. This synthesis could be generalized to prepare other lanthanide-oxide nanocrystals, which are of great importance to applications such as high-performance luminescence devices, magnets, catalysts, and other functional materials based on the optical and electronic properties arising from the 4-f electrons.

Acknowledgment. This work was supported by the University of Florida. We thank Charles R. Martin for helpful discussions and Kerry Siebein and Valentin Craciun for technical assistance.

Supporting Information Available: Additional TEM images (PDF). This material is available free of charge via the Internet at http://pubs.acs.org.

References

(1) (a) Alivisatos, A. P. *Nat. Biotechnol.* **2004**, *22*, 47. (b) Hu, J.; Odom, T. W.; Lieber, C. M. *Acc. Chem. Res.* **1999**, *32*, 435. (c) Lee, S. B.; Mitchel, D. T.; Trofin, L.; Nevanen, T. K.; Söderlund, H.; Martin, C. R. *Science* **2002**, *296*, 2198. (d) Kazes, M.; Lewis, D. Y.; Ebenstein, Y.; Mokari, T.; Banin, U. *Adv. Mater.* **2002**, *14*, 317.
(2) Han, M.; Gao, X.; Su, J. Z.; Nie, S. *Nat. Biotechnol.* **2001**, *19*, 631.
(3) Xia, Y.; Yang, P.; Sun, Y.; Wu, Y.; Mayers, B.; Gates, B.; Yin, Y.; Kim, F.; Yan, H. *Adv. Mater.* **2003**, *15*, 353.
(4) (a) Peng, Z. A.; Peng, X. *J. Am. Chem. Soc.* **2001**, *123*, 1389. (b) Lee, S.-M.; Jun, Y.-W.; Cho, S.-N.; Cheon, J. *J. Am. Chem. Soc.* **2002**, *124*, 11244. (c) Sun Y.; Xia Y. *Science* **2002**, *298*, 2176.
(5) Manna, L.; Milliron, D. J.; Meisel, A.; Scher, E. C.; Alivisatos, A. P. *Nat. Mater.* **2003**, *2*, 382.
(6) (a)Puntes, V. F.; Zanchet, D.; Erdonmez, C. K.; Alivisatos, A. P. *J. Am. Chem. Soc.* **2002**, *124*, 12874. (b) Chemseddine, A.; Moritz, T. *Eur. J. Inorg. Chem.* **1999**, *2*, 235. (c) Sigman, M. B.; Ghezelbash, A.; Hanrath, T.; Saunders, A. E.; Lee, F.; Korgel, B. A. *J. Am. Chem. Soc.* **2003**, *125*, 5638. (d) Ghezelbash, A.; Sigman, M. B., Jr.; Korgel, B. A. *NanoLett.* **2004**, *4*, 537. (e) Jin, R.; Cao, Y. C. Hao, E.; Mtraux, G. S.; Schatz, G. C.; Mirkin, C. A. *Nature* **2003**, *425*, 487. (f) Chen, S.; Carroll, D. L. *NanoLett.* **2002**, *2*, 1003. (g) Hao, E.; Kelly, K. L.; Hupp, J. T.; Schatz, G. C. *J. Am. Chem. Soc.* **2002**, *124*, 15182.
(7) Wyckoff, R. W. G. *Crystal Structures*, 2nd ed.; John Wiley & Sons: New York, 1964; Chapter 5.
(8) (a) Pan, Z. W.; Dai, Z. R.; Wang, Z. L. *Science* **2001**, *291*, 1947. (b) Urban, J. J.; Yun, W. S.; Gu, Q.; Park, H. *J. Am. Chem. Soc.* **2002**, *124*, 1186.

JA0481676